Optical coherence imaging of infarcted myocardium by biofunctionalized gold nanoshells

T. Muñoz Ortiz, Hu Jie, D. Ortgies, P. Paula Zamora-Pérez, S. Shrikhande, M. Granado, A.L. Villalon, E. Martín-Rodríguez, F. Alfonso, J. García Solé, Pilar Rivera, F. Rivero, and Daniel Jaque.

Fluorescence Imaging Group, Universidad Autónoma de Madrid, Madrid 28049, Spain

Nanobiology Group, Instituto Ramón y Cajal de Investigación Biosanitaria, Hospital Ramón y Cajal, 28034 Madrid, Spain.

Integrative Biomedical Materials and Nanomedicine Lab, Department of Experimental and Health Sciences (DCEXS), Pompeu Fabra University (UPF), PRBB, Barcelona 08003, Spain

Department of Cardiology, Hospital Universitario de la Princesa, Instituto Investigación Sanitaria Princesa (IIS-IP), Universidad Autónoma de Madrid, Calle Diego de León, 62, Madrid 28006, Spain

ABSTRACT: The unique combination of physical and optical properties of silica (core)/gold (shell) nanoparticles (gold nanoshells) makes them especially suitable for biomedicine. Gold Nanoshells have been used from high-resolution in vivo imaging to in vivo photothermal tumor treatment. Furthermore, the reduced size and large scattering cross section of Gold Nanoshells in the second biological window (1000-1700 nm) make them also especially adequate for molecular optical coherence tomography (OCT). In this work, we demonstrate how, after adequate functionalization, gold nanoshells in combination with clinical OCT systems are capable of imaging damage in the myocardium after an infarct. Since both inflammation and apoptosis are two of the main mechanisms underlying myocardial damage after ischemia, such damage imaging is achieved by endowing Gold Nanoshells with selective affinity for the inflammatory marker Intercellular Adhesion Molecule 1 (ICAM-1), and the apoptotic marker phosphatidylserine (PS). The results here presented constitute a first step towards a fast, safe, and accurate diagnosis of damaged tissue within infarcted hearts at the molecular level by means of the highly sensitive OCT interferometric technique.

Introduction.

Imaging of damaged myocardial tissues constitutes a valuable prognostic tool for patients with ischemic heart disease. Localization of myocardial damage is typically achieved by using either magnetic or nuclear contrast agents. Some of them (such as those containing gadolinium) are contraindicated to patients with renal impairment whereas others (such as XX) implies the use of ionizing radiation that could lead to the appearance of undesirable collateral effects. In order to avoid those limitations new biocompatible contrast agents not dealing with ionizing radiation are being developed for myocardium imaging. These include optical nanoparticles (NPs) capable of absorbing, scattering, or emitting infrared light. The good penetration of infrared light int tissues allows for high resolution deep imaging. In addition, the non-ionizing character of infrared light minimizes the collateral effects caused by imaging experiments. Of special relevance are Gold NPs (AuNPs) due to their unique combination of properties including excellent long-term stability, low toxicity, fast and cheap synthesis, facile surface biofunctionalization and potential tailoring of optical properties through rationale selection of shape and size. The geometry-dependent plasmon resonance of AuNPs lead to an enhanced optical response at selected wavelengths that have been extensively used in pre-clinical research. AuNPs have been recently used for cardiovascular studies making possible, for instance, visualization of atherosclerotic plaques, imaging of brain vasculature, thrombus photoacoustic detection, angiogenesis monitoring, drug delivery to myocardium tissues and enhancement of myocardium regeneration. It has been recently demonstrated how adequate biofunctionalization provides Au-NPs efficient targeting to damaged myocardium tissues. Indeed, visualization of myocardial scare has been demonstrated by using the Au-NPs as contrast agents in computed tomography. Au-NPs have also emerged as an efficient contrast agents in intracoronary Optical Coherence Tomography (OCT) that would make possible the replacement of ionizing radiation by infrared light thus minimizing possible adverse effects.

Among the great variety of Au-NPs, Gold nanoshells (GNSs) appear to be especially adequate for OCT imaging. When compared to gold nanoparticles of different geometries (nanorods, nanostars, nanocages) recent publications demonstrated that GNSs provides a superior optical extinction coefficient per mass of gold. This constitutes an advantage since it would require a reduced administration dose. Furthermore, it has been also postulated that spherical nanoparticles could be specially indicated for *in vivo* molecular imaging. It has been stated that when administrated via blood flow, spherical NPs interact more efficiently with cells than other geometries (such as elongated NPs) because the latter are extended by the flow. In addition, GNSs combine their large scattering cross section with high photothermal conversion efficiency making possible also their use as contrast agents not only in conventional optical coherence tomography but also in photothermal optical coherence tomography. Finally, the clinical application of GNSs as therapeutic agents has been recently demonstrated supporting the feasibility of the close future application of GNSs as contrast agents in the clinics.

In this work the large infrared scattering cross section of Gold Nanoshells (GNSs) combined with state-of-the art intracoronary OCT systems have been used for the visualization of damaged myocardium after an ischemic event. Selective accumulation of GNSs at damaged myocardium has been achieved by surface decoration providing them high affinity to miocardiocyte cells subjected to inflammation and apoptosis.

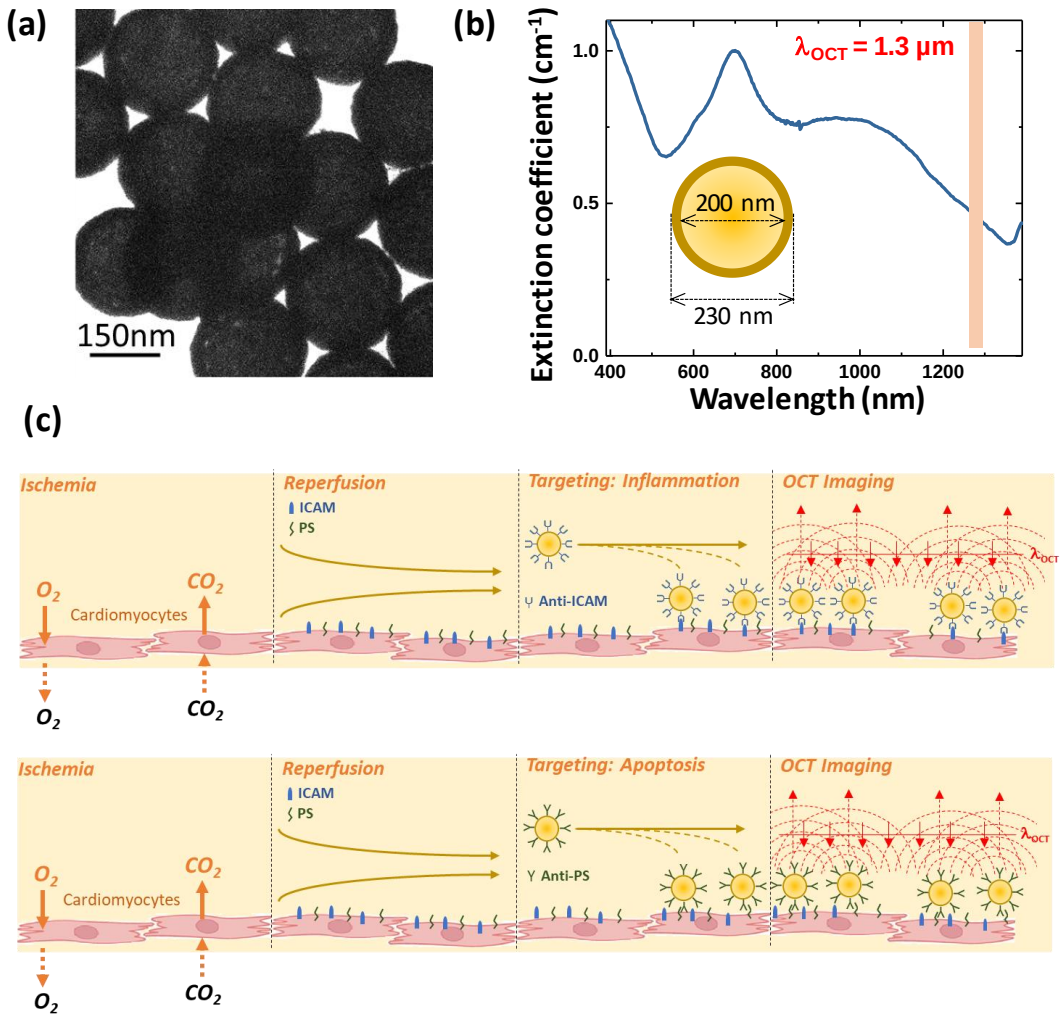

Figure 1.- (a) TEM image of the Gold Nanoshells used all along this work. **(b)** Extinction spectrum of the GNSs used in this work. The operating wavelength of the intravascular OCT system used in this work is also indicated. **(c)** Schematic representation of the use of functionalized Gold Nanoshells for molecular imaging of damaged cardiomyocytes in a ischemic event by Optical Coherence Tomography (OCT).

2. Methods.

2.1.- Bio-functionalized Gold Nanospheres.

In this work we used GNSs provided by Nanocomposix. **Figure 1(a)** shows a typical TEM picture of the GNSs revealing their homogeneous size distribution as well as their spherical shape. They consist of a 200 nm diameter silica core surrounded by a 15 nm thick gold shell (see schematic drawing in the inset of **Figure 1(b)**). These GNSs show a broad plasmonic band extending from visible up to the infrared that leads to a high extinction coefficient at the operating wavelength of cardiovascular OCT systems (1300

nm as indicated in **Figure 1(b)**). These particular GNSs were selected for our study as previous works demonstrated their optimum performance as contrast agents for intracoronary OCT in comparison with other Au-NPs.

Any ischemic event cases both inflammation and apoptosis in micardiocyte cells due to the transient reduction of oxygen supply that results in an upper-regulation of both the intercellular adhesion molecule (ICAM) and the phosphatidylserine encyme (PS). Thus, in order to provide our GNSs with adhesion affinity to the damaged myocardium tissues we decorated their surfaces with either anti-ICAM peptide or with anti-PS antibody (see the schematic representation of **Figure 1(c)**).

For anti-PS biofunctionalization we used GNSs at a initial concentration of 0.05mg/ml (8.5 x 108 particles/ml), carboxy thiolated PEG (CT-PEG 12) from Thermo Scientific was with a MW 634.77 and stock concentration 0.105M, and PEG dissolved using 1.5ml MilliQ. EDAC buffer was prepared using 2% w/v EDC and 3% w/v NHS in PBS and anti-phosphatidylserine from Merck Milipore (1mg/ml) was used. We first proceed with the PEGylation of gold nanoshells according to the following steps: i) 1. 5 ml CT-PEG diluted in MiliQ to give a final concentration of 0.01M was added to a glass vial containing 5ml GNS (0.05 mg/ml) under sonication in a 1:1 ratio. This mixture was sonicated for 5 minutes and magnetically stirred for 1 hour at room temperature with a speed of ~760 rpm. ii) PEGylated GNS transferred to an eppendorf tube and centrifuged at 5600 rpm for 10 minutes. The supernatant was discarded, the pellet washed with MiliQ and redispersed under sonication. The wash cycle was performed 3 times to remove excess PEG. Iii) The final pellet was redispersed using 5ml HBSS. 1 ml aliquot was removed for characterisation using Fourier Transformation Infra Red (FTIR) and Dynamic Light Scattering (DLS). After PEGylation we proceed with conjugating anti-phosphatidylserine with PEG-gold nanoshells using EDC according to the following steps: i) In a glass vial under a sterile fume hood, 4ml of the GNS-PEG was mixed with 400µl EDAC buffer. 40µl of anti PS was slowly added to this mix (1:0.1:0.01 ratio). ii) The solution was magnetically stirred at room temperature for 2 hours at a speed of ~760 rpm. iii) After 2 hours, the reaction was quenched with 80µl 1M hydroxylamine for 10 minutes. iv) The solution was transferred to 1ml eppendorf tubes and centrifuged for 10 minutes at 5600 rpm. The supernatant was discarded, the pellet washed with PBS and redispersed under sonication. The washing cycle was repeated 3 times. The final pellet was redispersed in a total of 5ml PBS and stored at 40 C. v) While scaling up the production of GNS-PEG-anti-PS, the same ratios of reagents as mentioned above were used.

The procedure followed for anti-ICAM functionalization is described next. The commercial dispersion of GNSs functionalized with lipoic acid (10 mL, 0.5 mg) in PBS was centrifuged (4000 rcf, 30 min) and washed 2x with DMSO (1.5 mL) and then carefully dispersed in DMSO (1.5 mL). N-hydroxysuccinimide (NHS; 5.66 mg, 49.18 µmol), followed by 1-Ethyl-3-(3-dimethylaminopropyl)carbodiimide (EDC; 5.98 mg, 38.55 µmol) were added to the mixture and careful sonication and stirring were alternated for 30 min. Afterwards, the dispersion was centrifuged (4000 rcf, 20 min), washed 2x with

DMSO (1.5 mL),the supernatant solvent was removed and the activated GNSs were dispersed in borate buffer (1.5 mL, pH 8) and sonicated. The cLABL peptide (cyclo(1,12)PenITDGEATDSGC 0.33 mg, 0.28 µmol) was added and after sonicating for 30 min the mixture was stirred over night before being quenched with a few drops of 1 M glycine and stirred for another 30 min. Finally, the mixture was centrifuged (4000 rcf, 30 min), washed twice with PBS (2 mL and 1.5 mL) and then carefully re-dispersed in PBS (1.5 mL).

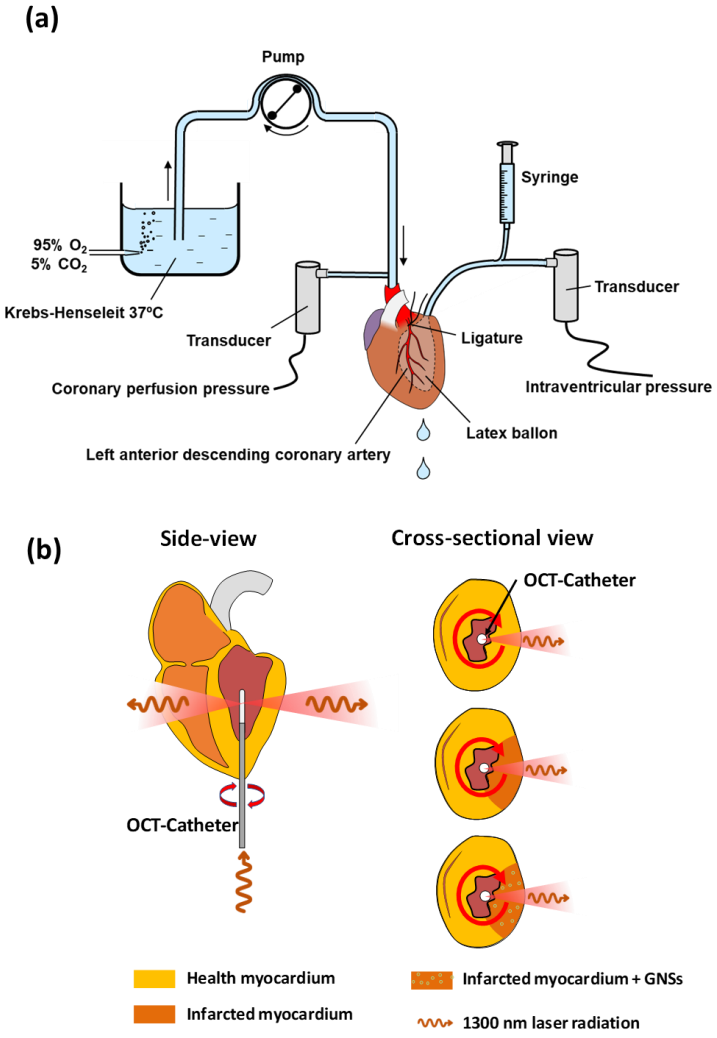

Figure 2.- (a) Schematic diagram of the experimental set-up used for the ex-vivo induction of an acute myocardial infarct in the heart of Sprague-Dawley rats using the Langendorff technique. **(b)** Side and cross sectional drawing of an infarcted heart in the presence of the OCT rotating catheter for molecular visualization of damaged myocardium. In the cross sectional views the cases of healthy or infarcted hearts after perfusion with vehicle or with a solution of Gold Nanoshells are represented.

2.2.- Langendorf model of infarcted heart.

Figure 2(a) shows an schematic representation of the Langendorff model adopted in this work. The hearts were removed from rats anesthetized with intra-peritonial injection of sodium pentobarbital (100 mg/kg) followed by an intra-venous injection of heparin

(1,000 UI). Retrograde perfusion (11-15 mL/min, 70 mmHg) of the heart with Krebs-Henseleit buffer (95% oxygen and 5% carbon dioxide) was performed through the cannulated aorta (pH 7.3). Coronary perfusion and left ventricular pressures were measured through a lateral connection in the perfusion cannula and a latex balloon, respectively. After 30 min of perfusion, partial ischemia was induced by ligation of the left anterior descending coronary artery. The artery was kept occluded during 15, 30, 45 or 60 min. After the ischemia, the ligation was removed and the hearth was subjected to 30 min of reperfusion. Finally, the perfusion system was modified to a closed circuit, in which a solution containing 1 mL of a colloidal dispersion of GNSs (0.035 mg/mL) was kept circulating for another 30 minutes. A control heart was also studied. In this case the same process was followed but without performing any artery occlusion. Finally, all animals used in this study were male as the estrous phase in female rats might affect the severity of ischemia-reperfusion. Indeed, it is reported that female gender favorably influences the remodeling and the adaptive response of the heart to myocardial infarction.

2.3.-Determination of PS and ICAM protein contents in infarcted hearts.

Total proteins were extracted from myocardial tissue by homogenization using a lysis buffer (RIPA). The total protein content was analysed by the Bradford method. For each western blot assay, resolving gels with SDS acrylamide (10%) were used and 100 µg of protein were loaded in each well. After electrophoresis, proteins were transferred to polyvinylidine difluoride (PVDF) membranes (Bio-Rad, Hercules, CA, USA) and transfer efficiency was determined by Ponceau red dyeing. The membranes were then blocked with Tris-buffered saline (TBS) containing 5% (w/v) non-fat dried milk and later incubated 4 °C overnight with XXXX. The membranes were subsequently washed and incubated with the corresponding secondary antibody conjugated with peroxidase (1:2,000; Pierce, Rockford, IL, USA). Peroxidase activity was visualized by chemiluminescence and quantified by densitometry using BioRad Molecular Imager ChemiDoc XRS System. All data were normalized to the housekeeping protein GAPDH and referred to % of control values on each gel.

2.4.- Imaging of myocardium infarcted tissues by Optical Coherence Tomography

The OCT system used all along this work is a commercially available cardiovascular OCT (CV-OCT) imaging system model Dragon-FlyTM (St. Jude Medical, St. Paul, MN, USA). Details about this system can be found elsewhere [10.1007/s12274-017-1674-4]. The CV-OCT system incorporates a compact super-luminescent diode operating at a central wavelength of 1320 nm with a bandwidth of 200 nm. The infrared laser radiation is coupled to a single mode fiber incorporated inside a 0.9 nm diameter catheter. The output end of the fiber is connected to a rotating reflector that deviates and scans the 1320 nm radiation in an orthogonal plane in respect to the fiber. The reflector also collects the back-scattered signal and couples it into the single mode fibre. The single-mode fiber is optically connected to an interferometer working in the frequency domain so that it can reconstruct cross sectional images at the position of reflector. The axial resolution of our CV-OCT system was approximately 15 µm, with a penetration length larger than 3 mm. For visualization of the damaged myocardium, the catheter was

introduced into the left ventricle of rats´ hearth after being subjected to the infract, as it is schematically represented in **Figure 2(b)**. In these conditions, the cross sectional images accounts for the OCT signal provided by both healthy and infarcted tissues. In presence of GNSs at the damaged myocardium tissues, the OCT intensity is expected to increase due to their high back-scattering cross section (**Figure 2(b)**).

3. Results and discussion.

Figure 3(a) shows the FTIR spectra corresponding to GNSs before functionalization (i.e. with only lipoic acid on their surface), to anti-ICAM functionalized GNSs and to anti-PS functionalized GNSs. Lipoic acid as a ligand presents the characteristic and broad O-H stretch vibration around 3425 cm^{-1}, a C=O stretch at 1676 cm^{-1} and the C-O vibration at 1085 cm^{-1}. After functionalization with the anti-ICAM the O-H peak has increased relative to the other bands due to the presence of more hydrogen bonding in the peptide. Additionally, the C=O double bond is shifted to 1646 cm^{-1}, which is typically observed when moving from the acid to the amide. Finally, the C-O vibration is drastically reduced in intensity, revealing a relative decrease in the presence of C-O, which also goes along with a shift from acid to amide. Finally, the GNSs functionalized with the anti-PS antibody present the typical bands for a protein: strong O-H band around 3400 cm^{-1}, strong band for C=O 1621 cm^{-1} and some stretching C-O band at 1065 cm^{-1}. Either the anti-ICAM or anti-PS surface decorations should make the targeting of damaged miocardiocytes as illustrated in **Figure 1**. As mentioned previously, previous works postulated the overexpression of both PS and ICAM in myocardium tissues after an ischemic event. In order to confirm such overexpression we have measured the PS and ICAM contents in hearts subjected to ischemic events of different durations. Results are shown in **Figure 3(b)** and **Figure 3(c)**. In both cases, experimental results reveal the expected overexpression of these two markers, but this seems to be weaker for the case of ICAM. Furthermore, it is possible to correlate a dependence of the overexpression magnitude with the duration of ischemic event. As a matter of fact it seems that longer inchemia events do not lead to significant increment in the content of neither PS not IAM proteins. This is at variance to the case of ATR1 protein (an excellent label of damaged cardiovascular tissues due to its overexpression after myocardial infection). Previous works have reported on an almost linear increment of ATR1 in infarcted hearts with the ischemia duration. Although we did not find a clear evidence that longer ischemia events lead to a larger concentrations of PS and ICAM proteins imaging experiments were carried out by using hearts subjected to 60 min ischemia events.

Figure 4 (a) includes the cross sectional OCT images corresponding to a control heart subjected to a 60 min ischemia. Control case corresponds to the infarcted heart prefunded with vehicle (i.e. with a solution without functionalized GNSs). The area affected by the ligation of the anterior descending coronary artery is indicated as “infarcted” area whereas the myocardium tissues not irrigated by the occluded artery are indicated as “healthy” tissue. In the control case, the OCT brightness obtained in the infarcted and healthy areas seem to be very similar. The similar OCT signal obtained from healthy and damaged myocardium in absence of GNSs is further evidenced in

Figure 4(b) that shows in-depth OCT intensity profiles obtained by averaging OCT signal over the dashed areas in **Figure 4(a)**, i.e. the OCT vs depth signal for both the healthy and infarcted myocardium tissues. In both cases the OCT intensity decreases monotonously with tissue depth as expected. In absence of any exogenous contrast agents, the OCT signal provided by a given tissue depends on its scattering and extinction properties. The larger OCT signal found in healthy tissues in the control heart suggests that the back-scattering coefficient of myocardium decreases due to the ischemic event. This is, indeed, in agreement with results published by D. Abookasis et al. who found that the wavelength-dependence of the reduced scattering (i.e., scatter power) of brain tissues decreases significantly after an ischemic event. Not only that, our findings are also in good agreement with the results published by S. Akter and co-workers who, using a single-reflectance fiber probe, found that the reduced scattering coefficient of liver decreased during an ischemic event. In our experimental conditions the variation in the OCT (back-scattered) signal was close to the intrinsic uncertainty of OCT measurements so that reliable detection of ischemic myocardium tissues requires the help of a contrast agents. In order to quantify the OCT intensity change at the ischemic event we define an integrated OCT signal:

$$I_{OCT} = \int I_{OCT}(z)dz \quad (1)$$

where $I_{OCT}(z)$ is the OCT intensity at depth z (ranging from 0 up t 2 mm). From the in-depth profiles included in **Figure 4(b)** we have estimated that the integrated OCT signal at the healthy and ischemic tissues are $I^{c}_{OCT}(Inf)$ = 0.80±0.07 and $I^{c}_{OCT}(health)$ = 0.77±0.06, respectively (**Figure 5(a)**). In $I^{c}_{OCT}(Inf)$ and $I^{c}_{OCT}(health)$, the superscript c stands for control. The normalized OCT contrast (ΔI^{norm}_{OCT}) can be defined as:

$$\Delta I^{norm}_{OCT} = \frac{I_{OCT}(Inf) - I_{OCT}(health)}{I_{OCT}(health)} \quad (2)$$

For the control hearth (i.e. without any contrast agent) we have obtained $\Delta I^{norm,c}_{OCT} \approx -3.7\%$ (**Figure 5(b)**). Thus, differences do exist between the healthy and infarcted tissues but they are small and close to the uncertainty of our OCT measurements. This clearly indicates that detection of infarcted tissues by using infrared OCT requires the use of contrast agents that would enhance the OCT signal difference between infarcted and healthy tissues.

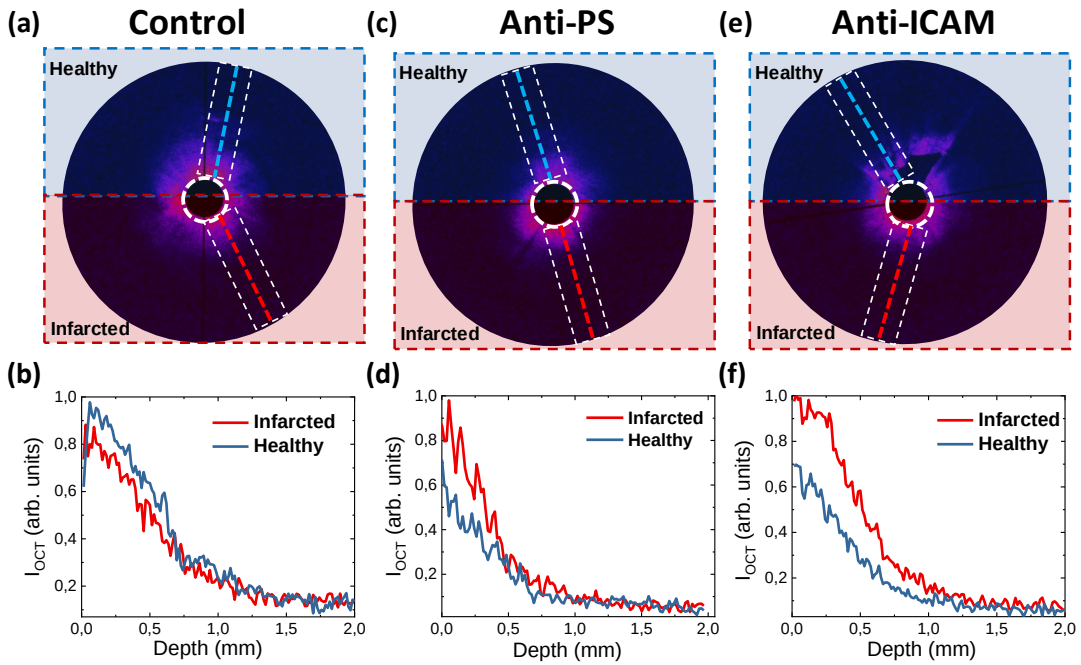

Figure 4. Cross sectional OCT images of a healthy heart (**(a)**) and infarcted hearts perfused either with anti-PS (Anti-PS, **(c)**) or anti-ICAM (Anti-ICAM, **(e)**) functionalized GNSs during reperfusion. **(b)**, **(d)** and **(f)** show the depth profile of the averaged OCT signal calculated from the analysis of the OCT signal over the dashed rectangles included in (a), (c) and (e).

Figure 4(c) shows the cross-sectional image of an infarcted heart subjected to a perfusion with anti-PS functionalized GNSs. In this case the infarcted tissue shows a larger OCT signal indicating an enhanced back-scattering of infrared light. This is further evidenced in **Figure 4 (d)** that includes the OCT intensity profiles as obtained from both healthy and infarcted tissues (profiles have been obtained by averaging the OCT signal in the dashed boxes indicated in **Figure (c)**. We attribute the larger OCT signal to the presence of anti-PS functionalized GNSs and to their high scattering cross section at the OCT wavelength. In this case, the OCT signal accounts for the back-scattering signal generated by tissues plus that generated by GNSs adhered to the damaged cardiomyocytes. Such adhesion reveals the cell damage (apoptosis) caused by the 60 min ischemic event. Note that the perfusion with anti-PS functionalized GNSs overcome the OCT intensity reduction observed for ischemic tissues in control hearts. From experimental data of **Figure 4(b)** lead to $I_{OCT}^{PS}(Inf)$ = 0.99±0.08 and $I_{OCT}^{PS}(health)$ = 0.81 ±0.07, where the subscript PS stands for the anti-PS functionalization (**Figure 5(a)**). The normalized OCT contrast as defined in expression (2) is $\Delta I_{OCT}^{norm,PS} \approx +22\%$. Note that the presence of the GNSs at damaged tissues has turned the normalized OCT contrast from negative in control to positive.

Finally, **Figure 4(e)** corresponds to the cross sectional image of a infarcted heart after being subjected to a reperfusion with anti-ICAM functionalized GNSs. **Figure 4(f)** shows the averaged in-depth profiles of the OCT intensity as obtained from both healthy and infarcted tissues. Again, the perfusion with functionalized GNSs lead to a clear

enhancement of the OCT signal generated at the infarcted myocardium tissues in respect to the healthy one. As a matter of fact, experimental data included in Figure 4(f) lead to $I_{OCT}^{IC}(Inf)$ = 1.05±0.09 and $I_{OCT}^{IC}(health)$ = 0.79 ±0.06, where the subscript IC stands for the anti-ICAM functionalization (**Figure 5(a)**). The normalized OCT contrast as defined in expression (2) is $\Delta I_{OCT}^{norm,IC} \approx +32\%$. (**Figure 5(b)**) Thus, it seems that anti-ICAM functionalization results more efficient for targeting the infarcted miocardyum than anti-PS. Although further experiments, including in vivo, would be necessary to verify this conclusion, it seems that targeting inflammation could be a better strategy for infarcted myocardium imaging than targeting apoptosis.

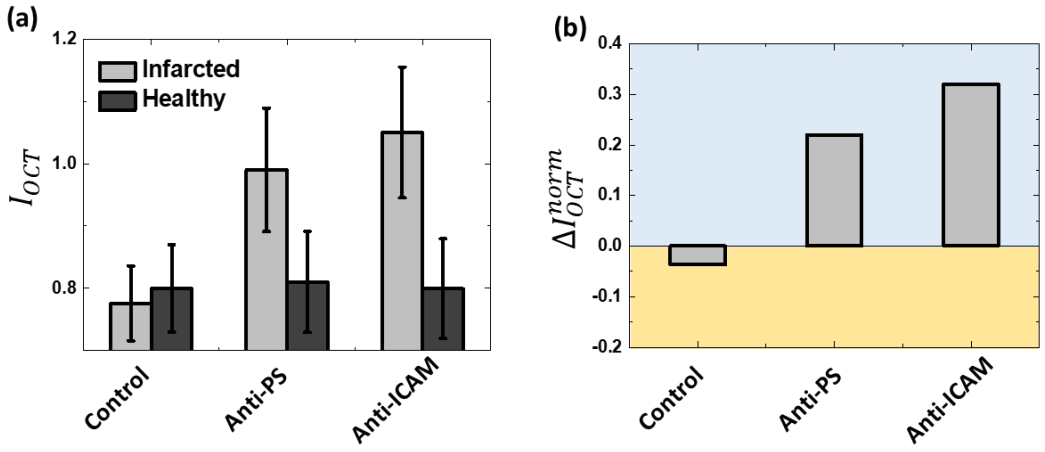

Figure 5. (a) Integrated OCT signal corresponding to healthy and infarcted myocardial tissues obtained from hearts submitted to an acute myocardial infarction (Infarcted) and perfused with a vehicle (control) and with a solution containing anti-Ps and ant-ICAM functionalized gold nanoshells during reperfusion. **(b)** Normalized OCT contrast between infarcted and healthy tissues as obtained from hearts submitted to an acute myocardial infarction (Infarcted) and perfused with a vehicle (control) and with a solution containing anti-Ps and ant-ICAM functionalized gold nanoshells during reperfusion.

4. Conclusions.

In summary, the ability of biofunctionalized Gold Nanoparticles for imaging of infarcted myocardium tissues has been explored. Two different strategies have been followed: targeting inflammation and apoptosis events, both taking place simultaneously in cardiomyocytes after an ischemic event. For that purpose, Gold Nanoshells have been functionalized in order to provide them specific affinity to the cardiomyocytes overexpressing either the intercellular adhesion molecule (ICAM) and the phosphatidylserine enzyme (PS). Ex vivo results demonstrate the ability of both functionalizations to induce selective accumulation of Gold Nanoshells at damaged myocardium tissues. Such selective accumulation causes an enhancement in the bac-scattering efficiency and, therefore, makes the infarcted tissue visible by infrated intracoronary Optical Coherence Tomography.

Results here included constitute the first demonstration of molecular imaging of infarcted hearts by combining an already operating and approved technique

(intracoronary OCT) with an optical proble already being used at the clinics such as Gold Nanoshells. This work constitutes the first step towards fast and accurate diagnosis of infarcted heart by using non ionizing radiation and plasmonic nanoparticles.